EXPERIMENTAL EVALUATION OF THERMALS PERFORMANCES OF THE SOLAR DRYER WITH PARABOLIC TROUGH COLLECTOR

B. Magloire Pakouzou1[1,2*]; N. Landry M'Bouana1[1]; M. Thierry Ky[2]; Jean M'Boliguipa[1]; D. Joseph Bathiébo[2]*.

[1]*Carnot Laboratory of Energetics, Faculty of Sciences, University of Bangui, C.A.R*

[2]*Laboratory of Renewable Thermal Energies, University Ouaga1 Pr. J. K.Z., Burkina Faso.*

* Corresponding authors : mb.pakouzou@gmail.com, djbathiebo@gmail.com

Abstract: A cylindrical-parabolic solar-thermal converter, with 0.5m^2 of capture surface, was manufactured and attached to a furnace, constituting an indirect solar dryer. Thermal balances of the elements of the receiver, housed in the focal point of this collector, are established. A campaign of vacuum tests of this dryer indicated temperatures of the heat-bearing air in natural convection, along the absorber tube (70°C) and inside the drying cage (almost 60°C, on average). The average thermal efficiency of said converter has been evaluated at 50%. The higher the efficiency, the less the converter's capture surface is required and, therefore, less investment is required. These promising results testify to the effective performance of this new dryer compared to dryers with flat collectors, whose efficiencies could not exceed 40% despite the large surface area of these collectors.

Keywords: Performance-Thermal, Solar-Dryer, Cylindro-Parabolic, efficiency.

NOMENCLATURE

☞ LATIN LETTERS

A_i : area of a slice [m^2].

C_i : specific heat [J.kg^{-1}.K^{-1}].

D_i : diameters [m]

d_z : length of a slice [m]

G : Solar irradiation [W.m^{-2}]

h_i : transfer coefficients [W.m^{-2}.K^{-1}].

q_a : absorbed flux [W/m].

q_b : solar irradiation absorbed by the glass

q_{in} : energy exchanged through the air confined between the absorber and the glass [W.m^{-1}].

q_m : mass flow rate [kg.s^{-1}].

q_{out} : heat exchanged between the glass cover and the external environment

q_v : volume flow [m^3.s^{-1}].

q_w : flow gained by the fluid [W.s^{-1}].

T_i : Temperatures [K]

t : time[s]

☞ GREEK LETTERS

α : absorptivity [%],

β : thermal expansion coefficient [1/K]

δ : angle [rad]

ε : emissivity [%]

θ : angle[rad]

λ_a : thermal conductivity coefficient [W.m^{-1}.K^{-1}]

ν : kinematic viscosity [m^2.s^{-1}]

ρ_i : densities [kg.m^{-3}]

σ : Stefan's constant [W.m^{-2}.K^{-4}]

τ : transmitivity [%]

φ_i : heat flow [W]

1. INTRODUCTION

In the literature, extensive studies have been carried out to improve the performance of indirect flat plate solar dryers, including : Dissa et al [1] have proposed an indirect solar dryer, with a flat plate collector with dimensions 2.02m×0.85m, where the air circulation in the collector is not free, but provided by a fan. Abene A. et al [2] measured the drying time of grapes to the required moisture content with a constant air flow rate, without obstacles in the flat plate collector is 13h20min and with transverse-longitudinal obstacles in the collector is 5h50min. Introduction of obstacles in the air channel is an important factor for improvement of collector performance which in turn reduces the drying time of grapes. In order to improve the efficiency of the thermal exchanges between air and glass on the one hand and between air and absorber on the other, Malénguinza S. (2012) [3] proposed an indirect solar dryer with double-glazed flat plate collectors. The temperature of the air circulating inside the said collector is of the order of 57°C. But the radiation that has passed through several panes of glass weakens energetically, so the multiplication of panes of glass decreases the overall transparency of the glass. Dianda et al (2015) [9] fixed straight fins on a flat absorber with an area of $3m^2$ and found an improvement of about 20% in thermal efficiency.

Of the above, the temperature level of the drying air and the drying time in these dryers are the key parameters to be optimized.

Thus, the parabolic trough solar dryer is a suitable system, which avoids the cost of improving the thermal performance of a flat plate solar dryer [4]. Experimental tests of this dryer have been carried out. The results obtained and presented in this paper seem promising compared to data from other excavations.

2. PRESENTATION OF THE PARABOLIC CYLINDRICAL COLLECTOR DRYER

An indirect solar dryer, with a parabolic cylinder collector, was built at the Laboratoire d'Energies Thermiques Renouvelables, Université Ouaga 1 Pr J.K.Z (Burkina Faso), [4]. It consists of two essential linked parts: the parabolic cylinder collector placed upstream of the drying cage, in the focal point of which a coaxial tubular receiver is housed, and the oven, where the products to be dried are spread out on racks arranged in a rack one after the other. Figure 1 shows a photo of the experimental set-up.

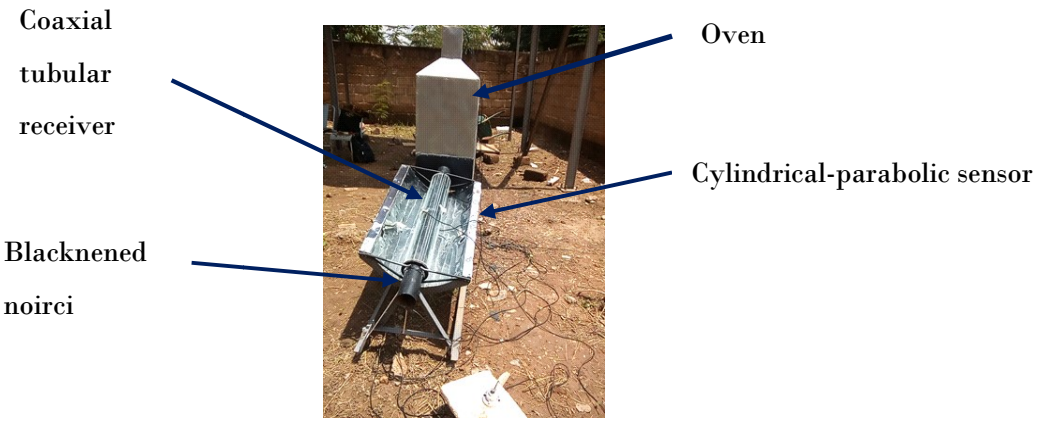

Fig. 1: Photo of the solar dryer with parabolic cylinder collector

3. OPERATION OF THE PARABOLIC CYLINDRICAL SENSOR DRYER

The present dryer is powered by a parabolic cylinder collector with a $0.5m^2$ collecting surface, whose general operating principle is to reflect the parallel rays of the sun, incident on its exposure surface, towards its blackened tubular absorber, placed in its focus. The absorber, 1m long, is wrapped with pieces of glass that are transparent and opaque to infrared ray, thus creating the greenhouse. This greenhouse, trapping in addition to the infrared rays of the direct radiation, is responsible for the increase of the temperature of the drying air, having a good evaporation power, both along the absorber and inside the drying chamber, thus favouring its natural flow.

Heat balances established hereafter have made it possible to write down the exchanges which take place between the components of the fundamental part (sensor) of the said dryer.

4. TRANSFER EQUATIONS

Thermal analysis is a fundamental step for the overall improvement of the efficiency of a solar system [4]. The different heat exchanges in the absorber are distributed as shown in Figure 2:

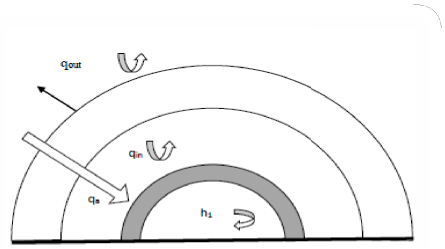

Fig.2 : Cross section of the heat transfer tube

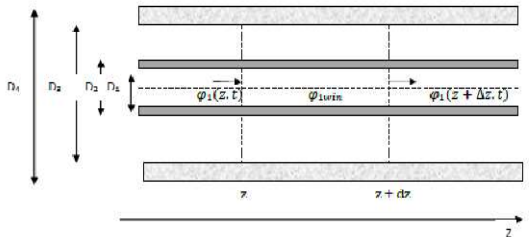

Fig.3 : Longitudinal section of heat transfer tube

- The heat balance of the medium at time t in the duct element dz at position z (Fig. 3) is given by the following equation [5]:

$$\rho_1 C_1 A_1 \frac{\partial T_1(z,t)}{\partial t} = -\rho_1 C_1 q_V \frac{\partial T_1(z,t)}{\partial z} + q_w(z,t) \quad \text{(eq.1)}$$

- The heat balance of the absorber is given by equation 2 [4]:

$$\rho_2 C_2 A_2 \frac{\partial T_2(z,t)}{\partial t} = \lambda_2 A_2 \frac{\partial T_2(z,t)}{\partial z} + q_a(z,t) - q_{in}(z,t) - q_w(z,t) \quad \text{(eq. 2)}$$

- Heat exchange between the glass, the absorber and the outside is by natural convection, with T3 (z, t) being the temperature of the transparent cover of the receiver. The heat exchange between the transparent cover and the environment is established by relation (3) [5, 4]:

$$\rho_3 C_3 A_3 \frac{\partial T_3(z,t)}{\partial t} = \lambda_3 A_3 \frac{\partial T_3(z,t)}{\partial z} + q_b(z,t) + q_{in}(z,t) - q_{out}(z,t) \quad \text{(eq.3)}$$

The detailed expressions of the heat exchanged between the components of the receiver are in appendix.

5. THERMAL EFFICIENCY OF THE SOLAR INVERTER

The performance of a solar system depends mainly on the efficiency of its converter (collector) [4]. Thus, the thermal efficiency of the concentrator, one of the parameters defining the performance of the present prototype, is defined according to the following equation [6]:

$$\eta = \frac{q_m C_p (T_{s,air} - T_{e,air})}{G.A_0} \quad \text{(eq. 4)}$$

6. ACTION AND DISCUSSION

6.1. Measuring Air Temperatures along the absorber

Type J thermocouples have been arranged at the inlet, middle and outlet of the absorber tube (Figure 1). Although it is the end of winter, the temperatures of the drying air recorded at the inlet of the drying cage are comfortably above 70°C. Figure 4 below gives an idea of the evolution of these temperatures as a function of time.

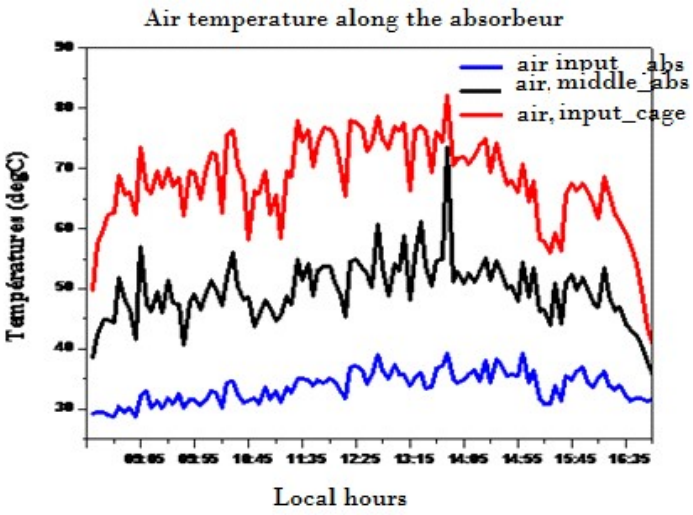

Fig. 4: Temperature of the drying air along the absorber tube

These temperatures vary according to the evolution of the global sunshine. They are regularly disturbed by alternating clouds and especially by the movement of the breeze. They naturally depend on the abscissa z along the absorber. They increase regularly from the inlet to the outlet of the absorber. This is due to the fact that the air, regularly heated by natural convection, rises inside the absorber tube and sees its temperature increase.

6.2. Air temperature inside the oven

The average temperature values measured on the first three racks, numbered from bottom to top, are 61.19°C, 58.65°C and 57.09°C respectively, with maxima equal to 75.2°C, 65.1°C and 63.2°C for each of the racks, spaced 10 cm apart inside the oven. The curves in Figure 5 give a better visualization of the temperature profile of the air inside the dryer enclosure.

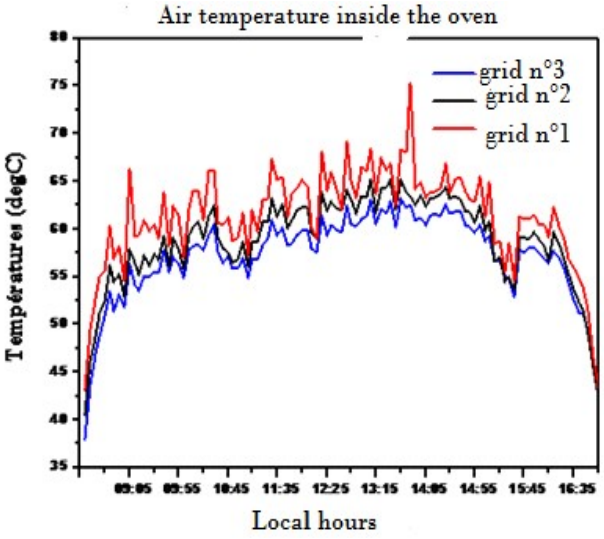

Fig. 5: Air temperatures through the racks

The data in the literature agree on the temperature range of 43.5°C to 60°C; for quality drying, ensuring better conservation of the nutrients in okra [7]. Our results are in perfect agreement with the literature, on the other hand, these results are compatible for the drying of okra. Also, the drying air exchanges with the inner wall of the kiln as it rises. This regularly lowers its temperature.

6.3. Absorber temperature profile

Two probes were placed in the middle and at the outlet of the absorber as shown in figure 1, thus raising its temperature and that of the drying air at the furnace inlet. The minimum and maximum values obtained were respectively equal to 40°C at the end of the day and 98.2°C at 12.05 hrs, in a test with load. The average value obtained is 87.22°C. However, values in excess of 100°C were also observed.

The temperature of the absorber also depends on its length, since the flow of the fluid by natural air convection along the tube is rising. Heat transfer by conduction, convection and the greenhouse effect between the glass pane and the absorber directly influences the thermo-physical characteristics of the heat transfer fluid.

The temperature of the drying air has been raised. It is still lower than the temperature of the absorber that provides the heat, as shown in figure 6.

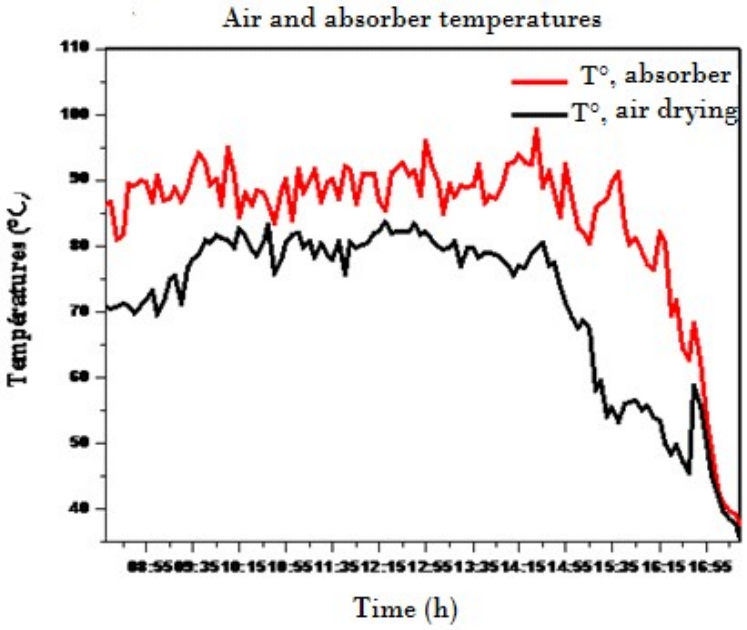

Fig. 6: Temperature development of the absorber and drying air

6.4. Concentrator performance profile

Figure 7 shows the experimental evolution of the concentrator's thermal efficiency as a function of time.

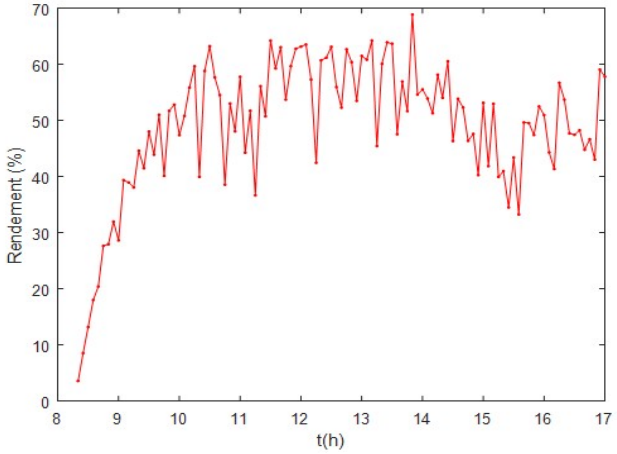

Fig. 7: Development of the thermal efficiency of the concentrator

The average thermal efficiency of the concentrator is around 50%. The manual tracking of the sun in its movement by the concentrator has allowed the incident solar beam to be parallel to the axis of the collector, so that the maximum of said rays is permanently focused on the receiver.

Around 5 p.m., the direct radiation decreases, but the thermal inertia of the receiver's material set allows the sensor to still produce large hot air flows. This results in an increase in efficiency at the end of the day, visible in this figure.

With regard to these values, we can say that the collector used here, with an opening of $0.5m^2$, seems quite efficient. Gama et al (2008) [12], with a parabolic cylindrical concentrator, with a $4m^2$ opening, obtained a maximum efficiency of 21% without solar tracking and of the order of 26.9% with solar tracking.

G. Ouédraogo (2017) [8], with a $4m^2$ flat plate collector, obtained between 10:30 am and 4:30 pm a thermal efficiency between 26% and 37%. B. Dianda (2015) [9], with a $3m^2$ flat plate collector, obtained an efficiency of 20%. In general, the thermal efficiency of a flat plate collector cannot exceed 40% [10].

But with a concentration converter, even a small one, one could hope for an efficiency exceeding 40%, as currently obtained!

The choice of such a sensor, with significantly reduced dimensions, is a technical-economic compromise [11, 12], above all an alternative to minimize the cost of the new dryer and therefore facilitates its acquisition.

7. VALIDATION OF THE CALCULATION CODE

In order to validate these results, the coolant air temperatures calculated using the code were compared with those measured experimentally. The assessment criterion chosen was to evaluate the square root mean systematic error, RMSE [4]. The agreement between these two temperatures is shown in Figure 8.

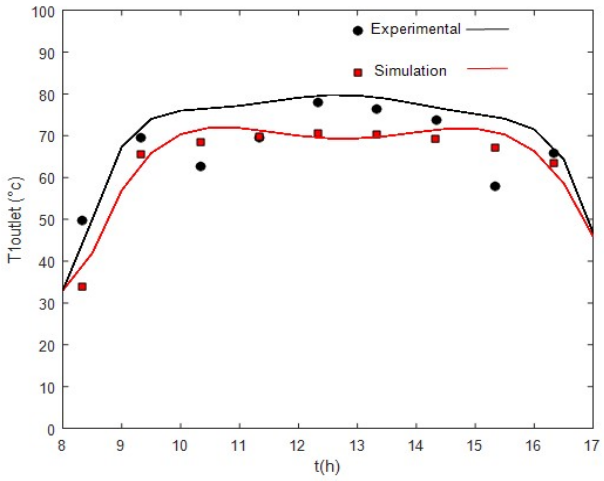

Fig. 8: Fluid temperature development at the inlet of the drying chamber

We then obtain on this figure: RMSE = $\sqrt{\frac{1}{N}\sum_{i=1}^{N}\left(T_{1,i}-T_{1,sim}\right)^2}$ = 4.5°C (eq. 5)

Quite a perfect harmony is noted!

Where $T_{1,i}$ and $T_{i,sim}$ are respectively the experimental and theoretical values of the air temperatures at the furnace inlet.

8. CONCLUSION

In this paper, experimental measurements of air temperatures along the absorber tube (70°C at the absorber outlet) and inside the furnace (almost 60°C, on average) of an indirect solar dryer, with a concentration collector, were carried out. The temperature level of the heat transfer air inside the drying cage is in accordance with the data in the literature for a quality drying of most of our agricultural products [7]. These measurements have made it possible to establish the effective thermal efficiency of a parabolic cylindrical converter, attached to the dryer housing. Also, the average thermal efficiency of this collector (50.23%), of rather small size (0.5m^2), confirms the thermal quality of the said converter, by comparison with the plane collector. The higher the efficiency, the less the collector surface is needed and therefore, less investments.

BIBLIOGRAPHY

[1]-**Dissa A.O., Desmorieux H., Bathiebo D.J. et Koulidiati J., 2011-**Estimation analytique et modélisation de la diffusivité d'eau au cours du séchage convectif de la mangue en considérant deux zones de diffusion. J. Soc. Ouest-Afr. Chim. 031, pp.21-34.

[2]-A**bene A., Dubois V., Le Ray M., 2004-** Study of a solar air flat plate collector, use of obstacles and application for the drying of grape. Vol.65, pp.15-22. Issue 1, jfoodeng.11.002, DOI:10.1016/j.2004.

[3]-**Malenguinza S., 2012-**Optimisation du capteur double vitrage par la méthode des plans d'expériences, thèse de doctorat, université d'Abomey Calavi, Bénin.

[4]-**Pakouzou B.M., Ky M. S. T., Gbembongo S. T., Ouedraogo G. P., Mackpayen O. A., Dianda B., Kam S., Bathiebo D. J., 2017-**Thermal performance of a receiver located in the caustic area of a cylindro-parabolic solar concentrator. Physical Science International Journal 16(3) : 1-14, 2017 ; PSIJ.37156 ; ISSN : 2348-0130. DOI : 10.9734.

[5]-**Chekirou W., Boukheit N. et Kerbache T., 2007-**Différents modes de transfert de chaleur dans un absorbeur d'un concentrateur solaire cylindro-parabolique. Revue des Énergies Renouvelables ICRESD-07, pp.21-28, Tlemcen.

[6]-**Pakouzou B. M., 2018**-Etude théorique et expérimentale d'un capteur cylindro-parabolique, annexé à une cage de séchage, these de doctorat, Université Ouaga 1 Pr J.K.Z, Burkina Faso.

[7]-**Pendre N. K., Prabhat K. Nema, Harsh P. Sharma, Rathore S.S. and Kush-wah., 2011-**Effet of drying temperature and slice size on quality of dried okra (Abelmoschus esculentus L. Moench). Journal of food Science and Technology.

[8]-**Ouedraogo G.W., 2017-**Étude numérique et expérimentale de l'écoulement de l'air en convection naturelle dans une tour solaire: Application au séchage du gombo. Thèse de doctorat, Université ouaga 1 Pr. J. KI-ZERBO.

[9]- **Dianda B., Ousman M., Kam S., Ky T. and Bathiebo D.J., 2015-**Experimental study of the kinetics and shrinkage of tomato slices in convective drying. African Journal of Food Science Vol.9 (5), pp.262-271, DOI: 10.5897/AJFS2015.1298 ISSN 1996-0794.

[10]-**Daguenet M., 1985-**Les séchoirs solaires: théorie et pratique. Publication Unesco, pp.456-476.

[11]-**Touati B., 2008-**Étude théorique et Expérimentale du Séchage Solaire des Feuilles de la menthe Verte. Thèse de doctorat de l'université de Tlemcen, Algérie.

[12]- **Gama A., Haddadi M. and Malek A., 2008-**Étude et réalisation d'un concentrateur cylindro-parabolique avec poursuite solaire aveugle. Revue des Énergies Renouvelables. Vol.11 N°3, pp.437-451.

[13]- **BEJAN A., 2004-**Convection heat transfer, John Wiley & Sons, ISBN 0-471-27150-0, New-York (USA).

ANNEX

Explicit expressions of the different flows

- **Heat balance between absorber and heat transfer fluid**

The heat received by the heat transfer fluid, at a date t in a unit dz, at the position z of the absorber tube (Figure 3), is given by the following equality:

$$\Delta Q_1(z,t) = \rho_1 C_1 A_1 \Delta z T_1(z,t) \quad \text{(A1)}$$

In fact,

$$\frac{\partial Q_1(z,t)}{\partial t} = \rho_1 C_1 q_V T_1(z,t) \quad \text{(A2)}$$

Thus, the heat balance of the fluid at time t in the duct element dz at position z is:

$$\frac{\partial(\Delta Q_1(z,t))}{\partial t} = \varphi_1(z+\Delta z,t) + \varphi_{1win}(z,t) \quad \text{(A3)}$$

With,

$\varphi_{1win}(z,t) = q_W \Delta z$: power gained by service air (A4)

$\varphi_1(z,t) = \frac{\partial Q_1(z,t)}{\partial t} = \rho_1 C_1 q_V T_1(z,t)$: power transferred to the fluid (A5)

$\varphi_1(z+\Delta z,t) = \rho_1 C_1 q_V T_1(z+\Delta z,t)$: power lost by the fluid (A6)

From then on, equality (A3) becomes:

$$\rho_1 C_1 A_1 \frac{\partial T_1(z,t)}{\partial t} = -\rho_1 C_1 q_V \frac{\partial T_1(z,t)}{\partial z} + q_w(z,t) \quad \text{(A7)}$$

q_w is calculated as follows:

-the first step is to calculate the Rayleigh number

$$Ra_1 = \frac{g\beta(T_2 - T_1)D_1^3}{\nu\alpha} \quad \text{(A8)}$$

-and then the Nusselt's number, depending on the geometry of the fluid flow, [13]

$$Nu_1 = 0.6(Ra * \sin\theta)^{0.25} \quad \text{(A9)}$$

Then comes the convective transfer coefficient between the inner wall of the absorber and the air.

$$h_1 = \frac{Nu_1 \lambda_a}{\nu\alpha} \quad \text{(A10)}$$

Thus, the heat is transferred to the heat transfer fluid by natural convection.

$$q_w(z,t) = h_1 \pi D_1 (T_2 - T_1) \quad \text{(A11)}$$

The solution, T1 (z, t), represents the variation in temperature of the drying air flowing through the conduit.

Thermal analysis of the absorber

In equation (2), where T_2 (z, t) is the temperature of the absorber, the flux absorbed, q_a, by the receiver slice dz is defined by:

$$q_a(z,t) = I \times (\rho\tau_3\alpha_2) \times C_g \times A_2 / dz \quad \text{(A12)}$$

and,

$$q_{in}(z,t) = \frac{2\pi K_{eff}}{\ln\left(\frac{D_3}{D_2}\right)}(T_2 - T_3) + \frac{\sigma\pi D_2\left(T_2^4 - T_3^4\right)}{\frac{1}{\varepsilon_2} + \frac{1-\varepsilon_3}{\varepsilon_3}\left(\frac{D_2}{D_3}\right)} \quad \text{(A13)}$$

$q_{in}(z,t)$ represents the energy exchanged by convection, assimilated to conduction with a correction coefficient, k_{eff} and by radiation respectively, through the air confined between the absorber and the glass pane.

The effective thermal conductivity of the air mass confined between the absorber and the glass (greenhouse effect) is given by,

$$k_{eff} = \max\left(1,\ 0.386 \times (\mathrm{Pr} \times Rac / (0.861 + \mathrm{Pr}))^{0.25}\right), \quad \text{(A14)}$$

- **Heat exchange between the glass, the absorber and the environment**

In equation (3), we have:

- q_{out}, amount of heat exchanged between the glass cover and the external environment

$$q_{out}(z,t) = h_4\pi D_4(T_3 - T_{amb}) + \varepsilon_3\pi\sigma D_4\left(T_3^4 - T_{amb}^4\right) \quad \text{(A15)}$$

- $q_b(z,t)$, being the solar irradiation absorbed by the glass.

$$q_b(z,t) = I \times (\rho\alpha_3) \times C_g \times A_3 / dz \quad \text{(A16)}$$